# J|A|C|S

## A R T I C L E S

# Enantioselective Separation on a Naturally Chiral Surface

Joshua D. Horvath,[†] Anjanette Koritnik,[†] Preeti Kamakoti,[†,‡] David S. Sholl,[†,‡] and
Andrew J. Gellman*,[†]

*Contribution from the Department of Chemical Engineering, Carnegie Mellon University,
Pittsburgh, Pennsylvania 15213, and National Energy Technology Laboratory,
Pittsburgh, Pennsylvania 15236*

Received July 25, 2004; E-mail: gellman@cmu.edu

***Abstract:*** Kinked-stepped, high Miller index surfaces of metal crystals are chiral and, therefore, exhibit enantiospecific properties. Previous temperature-programmed desorption (TPD) spectra have shown that the desorption energies of *R*-3-methylcyclohexanone (R-3-MCHO) on the chiral Cu(643)$^R$ and Cu(643)$^S$ surfaces are enantiospecific (*J. Am. Chem. Soc.* **2002**, *124*, 2384). Here, a comparison of the TPD spectra from Cu(111), Cu(221), Cu(533), Cu(653)$^{R\&S}$, and Cu(643)$^{R\&S}$ surfaces reveals that the enantiospecific desorption occurs from the chiral kink sites on the Cu(643) surfaces. Titration of the chiral kink sites with I atoms confirms this assignment of desorption features in the TPD spectra. Finally, the enantiospecific difference in the desorption energies of R- and S-3-MCHO has been used as the basis for demonstration of an enantioselective, kinetic separation of racemic 3-MCHO into its purified components during adsorption and desorption on the Cu(643)$^{R\&S}$ surfaces.

## 1. Introduction

Life on earth is based on chiral biomolecules such as enzymes, proteins, and DNA that are all of a single handedness. As a consequence, the left and right-handed enantiomers of chiral, bioactive compounds exhibit different physiological effects when ingested by living organisms. For example, while one enantiomer of a pharmaceutical can be therapeutic, the other can be toxic. Chiral bioactive compounds such as pharmaceuticals must, therefore, be produced enantioselectively using chiral environments with a preferred handedness: living organisms, chiral solvents, enantioselective chiral catalysts, etc. Enantioselective chemical production can be achieved either by using enantioselective processes to generate only one enantiomer or by using enantioselective methods to purify racemic mixtures of chiral compounds.

Surfaces have traditionally played an important role in many chemical processes including heterogeneous catalysis, adsorption, and separations. If such surfaces can be prepared such that they have either local or long-range chirality, they can serve as media for enantioselective adsorption and surface chemistry.[1-4] Common examples include the surfaces of stationary phases used for chromatographic separations.[5] Many are based on the immobilization of a chiral compound on an otherwise achiral substrate. Other examples of heterogeneous chiral media include metallic catalysts modified by the adsorption of a chiral species. In both examples, chirality is imparted to the surface by an adsorbed chiral modifier or template.

In addition to chiral surfaces created by the adsorption of chiral modifiers, one can identify surfaces with naturally chiral structures.[3,4,6] Many crystalline compounds have bulk structures that are chiral. Examples include quartz, calcite, and, of course, crystals of enantiomerically pure, chiral organic compounds. Cleavage of such crystals exposes crystalline surfaces that are also chiral with the chirality dictated by the chirality of the bulk. Although it may be somewhat counterintuitive, it is also possible for achiral crystalline materials to expose surfaces that are naturally chiral.[6] For example, although face centered cubic metals have highly symmetric, achiral bulk structures, surfaces such as Cu(643) and Cu(653) (Figure 1) with terrace-step-kink structures are naturally chiral. The kinks are formed by the intersection of (111), (110), and (100) microfacets, and their handedness arises from the clockwise, Cu($khl$)$^R$, or counterclockwise, Cu($khl$)$^S$, sense of progression from (111) to (100) to (110) microfacet.[7-9] These naturally chiral surfaces can, in principle, have the types of enantioselective properties needed for enantioselective chemical processing.[7,8,10-13]

---
[†] Carnegie Mellon University.
[‡] National Energy Technology Laboratory.

(1) Francotte, E. *Chim. Nouv.* **1996**, *14*, 1541.
(2) Baiker, A.; Blaser, H. U. *Handbook of Heterogeneous Catalysis*; VCH Publishers: New York, 1997; Vol. 4, pp 2422−2436.
(3) Hazen, R. M.; Filley, T. R.; Goodfriend, G. A. *Proc. Natl. Acad. Sci. U.S.A.* **2001**, *98*, 5487−5490.
(4) Hazen, R. M.; Sholl, D. S. *Nat. Mater.* **2003**, *2*, 367.
(5) Ahuja, S. *Chiral Separations by Chromatography*; Oxford University Press: Washington, DC, 2000.

---
(6) McFadden, C. F.; Cremer, P. S.; Gellman, A. J. *Langmuir* **1996**, *12*, 2483−2487.
(7) Attard, G. A. *J. Phys. Chem. B* **2001**, *105*, 3158−3167.
(8) Ahmadi, A.; Attard, G.; Feliu, J.; Rodes, A. *Langmuir* **1999**, *15*, 2420−2424.
(9) Sholl, D. S.; Asthagiri, A.; Power, T. D. *J. Phys. Chem. B* **2001**, *105*, 4771−4782.
(10) Horvath, J. D.; Gellman, A. J.; Sholl, D. S.; Power, T. D. *ACS Symp. Ser.* **2002**, *110*, 269−282.
(11) Horvath, J. D.; Gellman, A. J. *J. Am. Chem. Soc.* **2001**, *123*, 7953−7954.
(12) Horvath, J. D.; Gellman, A. J. *J. Am. Chem. Soc.* **2002**, *124*, 2384−2392.
(13) Attard, G. A.; Harris, C.; Herrero, E.; Feliu, J. *Faraday Discuss.* **2002**, *121*, 253−266.
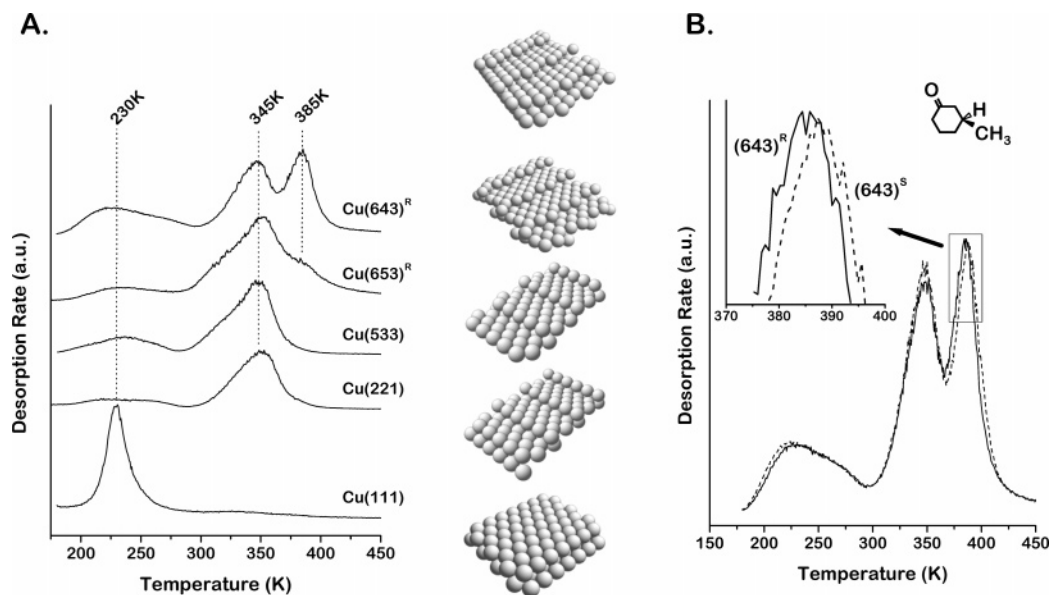
**Figure 1.** Temperature-programmed desorption spectra of R-3-MCHO from achiral and chiral Cu surfaces. (A) Desorption of R-3-MCHO from the Cu(111), Cu(221), Cu(533), Cu(653)$^R$, and Cu(643)$^R$ surfaces. The achiral Cu(111) surface has a hexagonal close-packed structure and exhibits a single desorption peak at 230 K. The achiral Cu(533) surface has (100) steps separated by (111) terraces and exhibits a desorption peak at 345 K from the steps and another broad desorption feature at 230 K arising from the terraces. Desorption from the Cu(221) surface with (110) steps and (111) terraces is almost identical to desorption from the Cu(533) surface. The Cu(643)$^R$ and Cu(653)$^R$ surfaces are chiral and have terraces, steps edges, and kinks. The desorption spectrum of R-3-MCHO from the Cu(643)$^R$ and Cu(653)$^R$ surfaces reveals peaks at 230, 345, and 385 K due to desorption from the terraces, steps, and kinks, respectively. (B) Desorption of R-3-MCHO from the kinks on the Cu(643)$^R$ and Cu(643)$^S$ surfaces. The enantiospecific difference in the peak desorption temperatures is $\Delta T_p = 3.5 \pm 0.8$ K.

There have been a number of experimental and theoretical studies of the surface chemistry of naturally chiral metal surfaces that reveal enantioselectivity. The earliest work, based on Ag(643)$^{R\&S}$ surfaces, simply showed that they have chiral structures.[6] Subsequent theoretical studies of the adsorption of chiral alkanes on a variety of chiral Pt surfaces suggested that the desorption energies of R- and S-chiral alkanes could differ by as much as $\Delta\Delta E_{des} = 5$ kJ/mol.[14] The first experimental observations of enantioselectivity on naturally chiral metal surfaces used electrochemical methods to show that the electro-oxidation rates of D- and L-glucose could differ by as much as a factor of 3 on chiral Pt(643)$^{R\&S}$ surfaces.[8] More recent work has revealed the enantiospecificity of the adsorption energies of *R*- and *S*-propylene oxide and R-3-MCHO on the chiral Cu(643)$^{R\&S}$ surfaces.[11,12] There is now clear evidence, based on a number of different experimental and theoretical methods, that naturally chiral metals surfaces do indeed exhibit enantiospecific surface chemistry.[7,9]

The most extensively studied chiral adsorbate–chiral surface pair is that of *R*-3-methylcyclohexanone (R-3-MCHO) adsorbed on the Cu(643)$^{R\&S}$ surfaces (Figure 1). The structure of the ideally terminated Cu(643)$^R$ surface is shown in Figure 1A and reveals kinked step edges separated by (111) terraces. This structure is not superimposable on its mirror image, and thus it is chiral.[6] Low-energy electron diffraction from Ag(643)$^{R\&S}$, Cu(643)$^{R\&S}$, and Pt(643)$^{R\&S}$ surfaces provides experimental verification of the fact that these surfaces do expose chiral structures.[6,10,15] In reality, one does not expect the ideal surface structures to exist due to the effects of thermal roughening which will cause a coalescence of the kinks along a step edge and possibly the coalescence of steps themselves. Simulations and

STM images of such surfaces show that this results in a reduction in the kink density and the production of kinks with a variety of local structures including some that cannot exist on the ideally terminated surface.[16–18] Nonetheless, recent STM images of R-3-MCHO adsorbed on the Cu(643)$^R$ surface at room temperature do reveal the presence of molecules aligned along step edges that run roughly along the [310] direction of the steps on the ideal Cu(643)$^R$ surface.[19] Previously published temperature-programmed desorption (TPD) spectra of R-3-MCHO adsorbed on the Cu(643)$^R$ surface at 150 K have revealed the three desorption features shown in Figure 1 at 230, 345, and 385 K.[12] Comparison with the desorption spectrum of R-3-MCHO from the Cu(111) surface has also indicated that the broad feature at 230 K must arise from molecules desorbing from the (111) terraces on the Cu(643)$^R$ surface. More importantly, comparisons of the desorption of R-3-MCHO from the Cu(643)$^R$ and Cu(643)$^S$ surfaces have revealed that the desorption feature at 385 K exhibits enantiospecificity. The peak desorption temperatures on the two surfaces differ by 3.5 ± 0.8 K, indicating that the R-3-MCHO has slightly different heats of adsorption on the two surfaces. Control experiments using racemic 3-MCHO reveal peak desorption temperatures at ∼385 K that were identical on the Cu(643)$^R$ and Cu(643)$^S$ surfaces. Thus, the differences observed in the desorption temperatures using R-3-MCHO must arise from a true enantiospecific effect.

The work presented in this paper adds significantly to our understanding of the enantiospecific adsorption of R-3-MCHO on the Cu(643)$^R$ and Cu(643)$^S$ surfaces. This work definitively assigns the three desorption features at 230, 345, and 385 K in the TPD spectra to desorption from the terrace, straight step

(14) Sholl, D. S. *Langmuir* **1998**, *14*, 862−867.
(15) Attard, G. A.; Ahmadi, A.; Feliu, J.; Rodes, A.; Herrero, E.; Blais, S.; Jerkiewicz, G. *J. Phys. Chem. B* **1999**, *103*, 1381−1385.

(16) Asthagiri, A.; Feibelman, P. J.; Sholl, D. S. *Top. Catal.* **2002**, *18*, 193−200.
(17) Giesen, M.; Dieluweit, S. *J. Mol. Catal. A* **2004**, *216*, 263−272.
(18) Power, T. D.; Asthagiri, A.; Sholl, D. S. *Langmuir* **2002**, *18*, 3737−3748.
(19) Zhao, X. Y.; Perry, S. S. *J. Mol. Cat. A* **2004**, *216*, 257.

edges, and the kinks, respectively. This indicates that, as one would expect, the enantiospecific desorption feature is the one associated with desorption from the chiral kink sites. In addition, infrared absorption is used to show that R-3-MCHO adsorbed at the kinks adopts an adsorption geometry that is enantiospecific or, in other words, depends on the chirality of the kink. Finally, we present the first evidence that one can use naturally chiral Cu(643)[R] and Cu(643)[S] surfaces to perform an enantioselective separation of a racemic mixture of 3-MCHO.

## 2. Experimental Section

All experiments were conducted in a stainless steel ultrahigh vacuum (UHV) chamber with a base pressure of less than $10^{-10}$ Torr. The chamber is equipped to perform $Ar^{+}$ ion sputtering, low-energy electron diffraction (LEED), Auger electron spectroscopy (AES), temperature-programmed desorption (TPD), and Fourier transform-infrared reflection absorption spectrometry (FT-IRAS). The chamber, the sample preparation, and the procedures used to make TPD measurements have all been described previously.[12]

Identification of the R-3-MCHO adsorption sites has been aided by the use of adsorbed iodine atoms to titrate adsorption sites on the surface.[20] Atomic iodine was deposited onto the Cu(643) and Cu(111) surfaces by adsorbing iodoethane onto a clean surface at approximately 100 K. Subsequent heating causes cleavage of the C−I bond in the adsorbed iodoethane, producing adsorbed atomic I and ethyl groups. This is followed by β-hydride elimination of the ethyl groups and, finally, desorption of ethylene and hydrogen at temperatures below 300 K.[21,22] Because atomic I is stable on Cu surfaces up to temperatures of roughly 900 K, this process leaves atomic I on the surface. The maximum iodine coverage attainable using this procedure is limited by the competition between adsorbed I and ethyl groups. Higher total iodine coverages were achieved by repeated cycles of first exposing the surface to 2 L (or less) of iodoethane and then heating to 300 K to desorb the ethyl groups as ethylene and hydrogen. Because ethylene and iodine are initially present on the surface in equimolar quantities, the cumulative ethylene desorption accurately quantifies the total iodine coverage on the surface. The saturated Cu(111) surface yielded a sharp low energy electron diffraction (LEED) pattern consistent with a $(\sqrt{3} \times \sqrt{3})R30°$ I adlayer.[23,24] Similar cumulative exposures of iodoethane were found to saturate the I coverage on Cu(643), although no ordered LEED pattern was observed from the I adlayer. Once atomic I was deposited to the desired coverage, the Cu(643) surface was cooled to 150 K, exposed to R-3-MCHO, and then heated at a constant rate to perform the TPD measurement.

The FT-IRAS measurements made use of a Mattson RS-1 spectrometer interfaced with the UHV chamber. The IR light was taken out of the spectrometer and introduced into the UHV chamber through a ZnSe lens/window that focused it onto the sample at grazing incidence. The reflected light was then collected by another ZnSe lens/window and focused by mirrors onto the HgCdTe narrow band detector. Spectra were taken using 5000 scans at a resolution of 4 cm$^{-1}$. Once the spectrum of the R-3-MCHO covered surface had been obtained, the sample was heated to 500 K to clean the surface and then cooled back to 120 K to obtain the background spectrum.

## 3. Theoretical

To determine the binding site for atomic I on the chiral surfaces, we investigated the adsorption of atomic I on a number

(20) Kamakoti, P.; Horvath, J.; Gellman, A. J.; Sholl, D. S. *Surf. Sci.* **2004**, *563*, 206−216.
(21) Jenks, C. J.; Bent, B. E.; Bernstein, N.; Zaera, F. *J. Phys. Chem. B* **2000**, *104*, 3008−3016.
(22) Jenks, C. J.; Bent, B. E.; Zaera, F. *J. Phys. Chem. B* **2000**, *104*, 3017−3027.
(23) Sung, D. Y.; Gellman, A. J. *Surf. Sci.* **2004**, *551*, 59−68.
(24) Dicenzo, S. B.; Wertheim, G. K.; Buchanan, D. N. E. *Surf. Sci.* **1982**, *121*, 411−420.
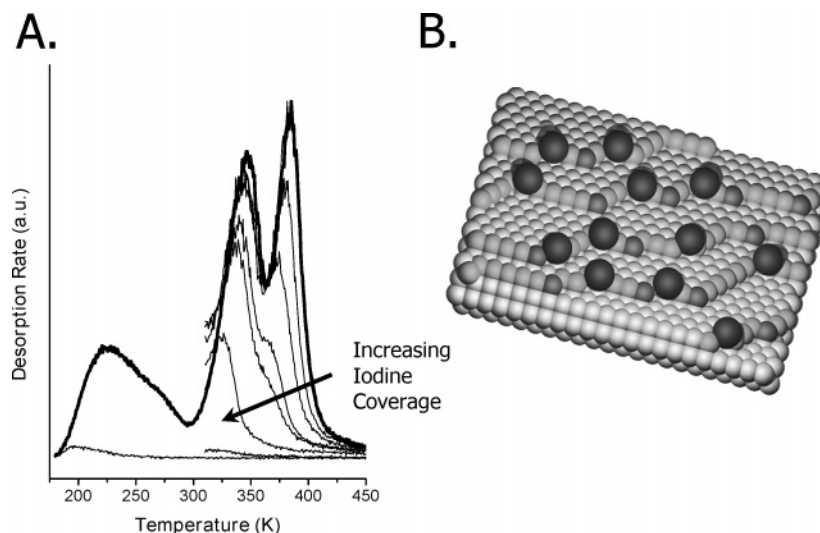
of Cu surfaces using density functional theory. The surfaces used included Cu(111), Cu(100), Cu(531), Cu(221), Cu(533), Cu(643), and thermally roughened non-Miller index surface related to Cu(643). All calculations were performed using the Vienna Ab initio Simulation Package (VASP) and procedures described elsewhere.[20] Adsorption energies were defined on the basis of the following expression for the dissociative adsorption of molecular iodine,

$$\Delta E_{ads} = E_{Cu} + \left(\frac{1}{2}\right)E_{I_2} - E_{I,ads}$$

where the terms on the right are the total energy of the bare Cu surface, gaseous $I_2$, and the Cu surface with an I adlayer, respectively. With this definition, more positive values of $\Delta E_{ads}$ indicate stronger binding of I to the surface.

## 4. Results and Discussion

**4.1. R-3-MCHO Adsorption Sites on Cu(643) and Cu(653).** At a coarse level of description, one can imagine that there are three types of adsorption sites for R-3-MCHO on the naturally chiral Cu surfaces: terrace, step edge, and kink sites. In reality, a thermally roughened surface exposes a variety of types of kinks, step edges with either (100) or (110) orientation, and a variety of terrace sites at different distances from the step edges.[16−18] One of the beautiful features of R-3-MCHO desorption from the chiral Cu(643) surface is that the three features in the desorption spectra shown in Figure 1 can be assigned uniquely to desorption from these three types of adsorption sites. The three desorption features occur at 230, 345, and 385 K. Figure 1 also shows the desorption spectra obtained following adsorption of a monolayer of R-3-MCHO on the Cu(111), Cu(221), Cu(533), and Cu(653)[R] surfaces. As shown previously, desorption from the Cu(111) surface occurs in the form of a narrow feature centered at 230 K, suggesting that the desorption feature at 230 K in the TPD spectrum obtained from the Cu(643) surface is due to desorption from the (111) terraces.[12] Most recently, TPD spectra have been obtained from monolayers of R-3-MCHO adsorbed on the Cu(533) and Cu(221) surfaces. These two surfaces expose straight (100) and (110) step edges separated by (111) terraces that are roughly four atoms wide. The TPD spectrum from the Cu(533) surface shown in Figure 1 reveals two features: a broad desorption peak centered at 230 K and a peak centered at 345 K. The TPD spectrum of a monolayer of R-3-MCHO from the Cu(221) surface is almost identical to that obtained from the Cu(533) surface. Empirically these TPD spectra suggest that the desorption peak observed at 345 K in the TPD spectrum obtained from the Cu(643)[R] surface is due to desorption from the straight portions of step edges. It is important to bear in mind that on a thermally roughened surface these are likely to be longer than the two atom wide step edges exposed by the ideal Cu(643) surface.[16,17] By elimination, these data suggest that the desorption peak at 385 K on the Cu(643)[R] surface must be due to molecules desorbing from the chiral kinks.

On the basis of the discussion above, one would expect that the TPD spectrum of R-3-MCHO from the Cu(653)[R] surface should look quite similar to that from the Cu(643)[R] surface. The difference in the ideal surface structures is simply in the nature of the kink sites. On the Cu(643) surfaces, the kinks are formed by the intersections of 2-atom (100) steps with 1-atom

**Figure 2.** Iodine atom titration of chiral 3-MCHO adsorption sites on a thermally roughened Cu(643)$^R$ surface. (A) Temperature-programmed desorption of R-3-MCHO monolayers from the Cu(643)$^R$ surface titrated with increasing initial coverages of adsorbed I atoms. The spectrum with the thick line was obtained from the clean Cu(643)$^R$ surface. The spectra shown with thinner lines were obtained from the surfaces with preadsorbed I atoms. They clearly reveal the initial depletion of R-3-MCHO desorption in the 385 K peak associated with molecules desorbing from the kink sites. (B) The simulated structure of a (643) surface that has been annealed to induce step roughening and the formation of kinks at the intersections of long step edges.[16,18] The steps are now long enough to accommodate 3-MCHO adsorption at the step edges as well as the kinks. Also shown are adsorbed I atoms at their preferred binding site at the kinks. The presence of I atoms at the kink sites blocks adsorption of R-3-MCHO.

(110) steps. On the Cu(653) surfaces, the kinks are formed by the intersections of 2-atom (110) steps with 1-atom (100) steps. Figure 1A shows that the desorption of R-3-MCHO from the Cu(653)$^R$ surface reveals the same three desorption features as desorption from the Cu(643)$^R$ surface. The most significant difference is that the apparent contribution from features associated with the kinks is significantly smaller on the Cu(653)$^R$ surface than on the Cu(643)$^R$ surface. As mentioned, these surfaces undergo thermal roughening, leading to coalescence of kinks along the step edges and thus a reduction in the kink density from that on the ideally terminated surfaces. Comparison of the TPD spectra on the Cu(643)$^R$ and Cu(653)$^R$ surfaces suggests that there is a higher degree of roughening on the Cu(653)$^R$ surface, resulting in a lower kink density. The (100) and (110) microfacets that form the kinked step have different relative energies, and thus it is not surprising that the Cu(643) and Cu(653) surfaces would roughen differently.[25]

To verify the assignment of the R-3-MCHO desorption features on the Cu(643) surfaces, we have performed a titration of the surface sites with atomic I. The idea is that if I atoms adsorb selectively at the kinks then they would be expected to selectively block the adsorption of R-3-MCHO at those sites. The deposition of I atoms has been accomplished as described elsewhere by the adsorption of ethyl iodide at 100 K followed by heating to 300 K.[20,23] This results in dissociation into I atoms and ethyl groups followed by $\beta$-hydride elimination of the ethyl groups and desorption of ethylene and hydrogen. The desorption yield of ethylene can be used to gauge the coverage of I atoms left on the surface.

The site for I atom adsorption has been determined by extensive DFT calculations.[20] Figure 2B depicts a thermally roughened (643) surface with I atoms adsorbed in their energetically most favorable sites. The thermally roughened surface has kinked steps separated by (111) terraces. The effect of roughening has been to coalesce kinks along the step edge

(25) Giesen, M.; Linke, U.; Ibach, H. *Surf. Sci.* **1997**, *389*, 264–271.

such that the density of kinks is reduced from that expected on the ideal (643) surface. Kinks are now formed at the intersections of long (100) and (110) step edges. This is consistent with the observation in the TPD spectra from the Cu(643)$^R$ and Cu(653)$^R$ surfaces in Figure 1 that reveal a significant amount of the R-3-MCHO desorbing from straight step edges. The DFT calculations of the energetics of atomic I adsorption at sites on the (111) terrace and at sites along both the (100) and the (110) step edges have revealed that the energetically favored binding site for atomic I is at the kink where the $\Delta E_{ads} = 174$ kJ/mol. The next most favored adsorption site is one Cu atomic diameter away from the kink along the (100) step edge and has a binding energy of $\Delta E_{ads} = 169$ kJ/mol. By comparison, the most favorable adsorption site on the terrace has a binding energy of only $\Delta E_{ads} = 145$ kJ/mol. Thus, not unexpectedly, at low coverages, I atoms on the Cu(643) surface are expected to adsorb at the kink sites as depicted in Figure 2B and thus block the adsorption of R-3-MCHO at the kinks.

The presence of adsorbed I atoms on the Cu(643) surface does indeed block the adsorption of R-3-MCHO. Figure 2A shows TPD spectra of R-3-MCHO from a Cu(643)$^R$ surface modified by adsorption of increasing amounts of atomic I. Following the adsorption of atomic I, the surface was exposed to 0.01 L of R-3-MCHO through a doser with the surface at 100 K. This exposure is sufficient to deposit one monolayer of R-3-MCHO on the clean Cu(643)$^R$ surface. The bold line in Figure 2A shows the TPD spectrum of one monolayer of R-3-MCHO from the clean Cu(643)$^R$ surface. The thinner lines are TPD spectra taken following adsorption of increasing coverages of atomic I and then exposure to 0.01 L of R-3-MCHO through a doser with the surface at 100 K. The initial effect of I adsorption at low coverages is to attenuate the intensity of the TPD feature at 385 K associated with desorption from the kink sites. As the atomic I coverage is increased, this desorption feature is almost completely eliminated before the onset of attenuation of the TPD peak at 345 K associated with molecules

desorbing from the straight step edges. Thus, titration of the Cu(643)$^R$ surface with atomic I confirms the assignment of the features in the TPD spectrum of R-3-MCHO from the clean Cu(643)$^R$ surface. The TPD peaks at 230, 345, and 385 K are due to R-3-MCHO desorption from the (111) terraces, straight step edges, and kinks, respectively.

If desorption from the kinks on the Cu(643)$^R$ surface occurs at 385 K, then one would expect to observe enantiospecificity in this feature when comparing desorption from the Cu(643)$^R$ and the Cu(643)$^S$ surfaces. This has been reported in earlier work and is illustrated in Figure 1B.[12] The difference in the peak desorption temperatures from the R- and S-kinks is $\Delta T_p = 3.5 \pm 0.8$ K. This corresponds to a difference in the adsorption energies of $\Delta \Delta E_{ads} \approx 1$ kJ/mol. Control experiments with racemic 3-MCHO indicate that this difference is due to a true enantiospecific effect. Desorption of R-3-MCHO from the Cu(653)$^{R\&S}$ surfaces should also be enantiospecific. Unfortunately, the peak at 385 K associated with desorption from the kinks on the Cu(653)$^{R\&S}$ cannot be resolved from the peak at 345 K associated with desorption from the straight step edges. As a consequence, despite our best efforts, it has not been possible to measure a peak desorption temperature with sufficient accuracy to demonstrate enantiospecificity on the Cu(653)$^{R\&S}$ surfaces.

**4.2. Enantiospecific Adsorbate Orientation on Chiral Surfaces.** The enantiospecific interaction of a chiral molecule with a chiral kink must, in principle, manifest itself in the structure or orientation of the molecule on the surface. In other words, the orientations of R-3-MCHO at R- and S-kinks should be different. Similarly, the orientations of R- and S-3-MCHO at an R-kink should be different from one another.

One of the most sensitive probes of molecular orientation on a metal surface is infrared absorption. Although the frequencies of vibrational modes in a molecule may not be very sensitive to molecular orientation, the intensities of infrared absorption are. For a given vibration mode with a dynamic dipole moment vector, $\vec{\mu}$, the intensity of infrared absorption is proportional to $(\vec{\mu} \cdot \hat{n})^2$, where $\hat{n}$ is the normal to the metal surface. Thus, the intensity of infrared absorption is proportional to $\cos^2 \theta_{\vec{\mu}\hat{n}}$, where $\theta_{\vec{\mu}\hat{n}}$ is the angle between the dynamic dipole moment vector and the surface normal. Thus, the absorption intensity is a very strong function of the angle between the two vectors and the orientation of the molecule on the surface.

Enantiospecific adsorption geometries are expected to be observed for molecules at the kinks on the Cu(643)$^{R\&S}$ surfaces. To isolate molecules to the kink sites only, the surfaces at a temperature of 320 K have been exposed to 0.15 L of R-3-MCHO through a doser and then cooled. At 320 K, desorption from the terraces and the straight step edges is rapid. As indicated by the TPD spectra in Figure 1, however, the molecules adsorbed at the kinks are stable. Figure 3 shows the FT-IRAS spectra of R-3-MCHO adsorbed on the Cu(643)$^{R\&S}$ surfaces at 320 K using an exposure sufficient to saturate the kink sites. It is quite apparent that, although the vibrational frequencies are not very sensitive to the chirality of the surface, the relative intensities of the absorption bands differ. Figure 3 also shows the vibrational spectrum of racemic 3-MCHO adsorbed at the kink sites on the Cu(643)$^R$ surface. Although it is not shown, the FT-IRAS spectrum of racemic 3-MCHO adsorbed at the kinks on the Cu(643)$^S$ surface is identical to
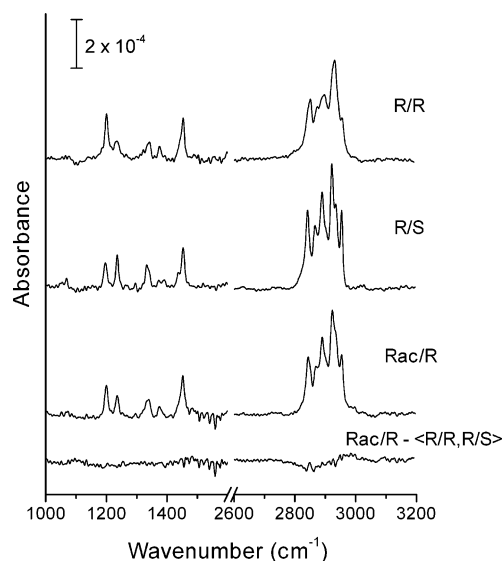


**Figure 3.** FTIR absorbance spectra of 3-MCHO selectively adsorbed at the kinks on the Cu(643)$^{R\&S}$ surfaces. Selective adsorption to saturate just the kinks was achieved by adsorption at 320 K followed by cooling to $T < 120$ K. The differences in the absorption intensities of the R-3-MCHO adsorbed at the kinks on the Cu(643)$^R$ surface, R/R, and at the kinks on the Cu(643)$^S$ surface, R/S, arise from enantiospecific differences in the adsorption geometry at the kinks. The FTIR spectra of the racemic mixture adsorbed selectively at the kinks are identical on both surfaces. The FTIR spectrum of the racemic mixture on the Cu(643)$^R$ surface, Rac/R, is identical to the average of the spectra of R-3-MCHO on Cu(643)$^{R\&S}$ surfaces, ⟨R/R,R/S⟩. This indicates that adsorption of the racemic 3-MCHO on Cu(643)$^R$ at 320 K fills half the kinks with R-3-MCHO and the other half with S-3-MCHO.

that on the Cu(643)$^R$ surface, as it should be. The final spectrum of Figure 3 shows the difference between the FT-IRAS spectrum of the racemic mixture and the average of the spectra of R-3-MCHO on the Cu(643)$^{R\&S}$ surfaces. The spectrum of the racemic mixture is just the average of the spectrum of the pure R-3-MCHO on the Cu(643)$^{R\&S}$ surfaces. Attempting to assign the vibrational bands and deduce the molecular orientation of the R-3-MCHO adsorbed at the kinks will not be discussed in this paper. The primary point of these spectra is to demonstrate that the orientations at the R- and S-kinks are indeed enantiospecific.

**4.3. Enantioselective Separation of Racemic 3-MCHO on Cu(643)$^{R\&S}$.** As shown above, the adsorption of R-3-MCHO on the Cu(643)$^{R\&S}$ surfaces is indeed enantiospecific. R-3-MCHO has a higher adsorption energy at the S-kinks than at the R-kinks, and this manifests itself in the form of different adsorption geometries and slightly higher desorption temperatures during TPD experiments. Differences in the adsorption energies of chiral compounds on chiral surfaces are the root of enantioselective chromatographic separations and can, in principle, be exploited to induce a separation of racemic 3-MCHO on chiral Cu(643)$^{R\&S}$ surfaces.

In principle, there are two types of adsorption-based separations: an equilibrium separation and a kinetic separation. In the case of an equilibrium separation, a surface is exposed to the racemic mixture of a chiral compound for a time sufficient to allow equilibrium to be reached between the adsorbed phase and the gas phase. The relative coverages of the two enantiomers at a given temperature and pressure will be dictated by their adsorption isotherms, $\theta(T,P)$, and their individual heats of adsorption. Under equilibrium conditions, the coverage of the
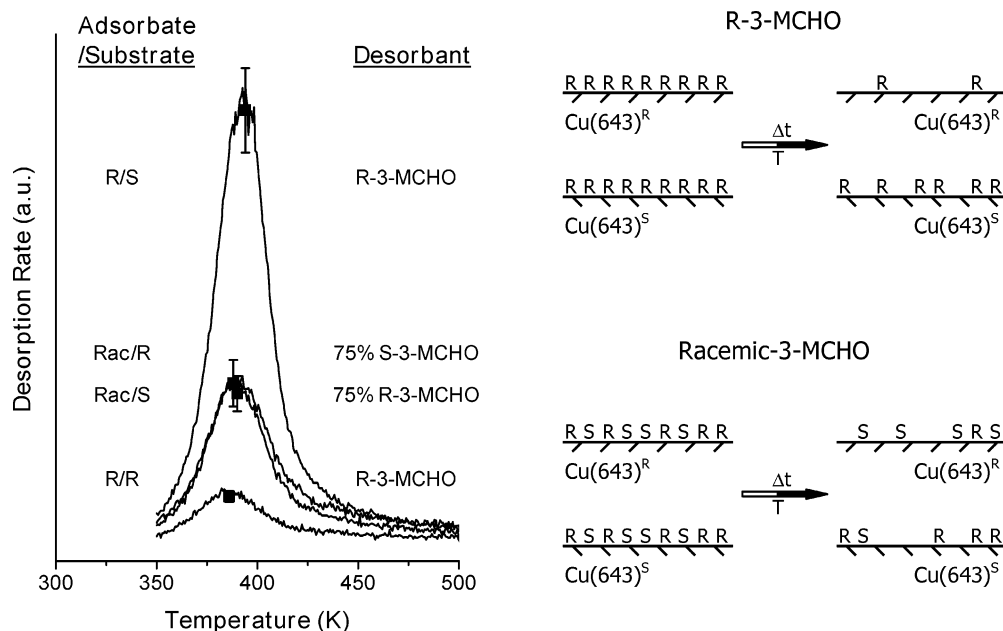
**Figure 4.** Kinetic separation of racemic 3-MCHO on the Cu(643)$^{R\&S}$ surfaces. The Cu(643)$^R$ and Cu(643)$^S$ surfaces were exposed to 3-MCHO at 360 K followed by heating at 360 K for 300 s to induce partial desorption. TPD spectra were obtained to determine the amount of 3-MCHO remaining on the surfaces. As shown in the upper right panel, exposure to R-3-MCHO followed by heating leaves a higher coverage of R-3-MCHO remaining on the Cu(643)$^S$ surface than on the Cu(643)$^R$ surface. The TPD spectra in the left panel reveal roughly 10 times the coverage or R-3-MCHO on the Cu(643)$^S$ surface, R/S, as on the Cu(643)$^R$ surface, R/R. As shown in the lower right panel, exposure of Cu(643)$^R$ to racemic 3-MCHO followed by heating at 360 K leaves a greater coverage of S-3-MCHO than R-3-MCHO on the Cu(643)$^R$ surface. The desorption spectra in the left panel reveal that, following exposure of the Cu(643)$^R$ surface to racemic 3-MCHO at 360 K and heating for 300 s, the coverage of 3-MCHO remaining is 4 times the coverage remaining after exposure of the Cu(643)$^R$ surface to R-3-MCHO. The excess must be due to excess S-3-MCHO, indicating that a separation has occurred.

enantiomer with the higher heat of adsorption will be greater than that of the other enantiomer. Rapid removal of the gas phase would result in a net purification of the racemic mixture by leaving an excess of one enantiomer adsorbed on the surface.

In a kinetic separation, the racemic mixture is adsorbed from the gas phase, and then the gas phase is removed prior to reaching equilibrium. At a given temperature, the two enantiomers of the adsorbed racemic mixture will desorb into the gas phase. Because the two enantiomers have different adsorption energies, their rates of desorption differ, and the one with the lower adsorption energy will desorb more rapidly. After a given period of time, the mixture on the surface is no longer racemic and is enriched in the enantiomer with the higher adsorption energy. This process is illustrated in the right-hand panel of Figure 4.

We have attempted a kinetic separation of racemic 3-MCHO on the Cu(643)$^{R\&S}$ surfaces. As illustrated by the FT-IRAS spectra of Figure 3, the initial exposure of racemic 3-MCHO to the Cu(643)$^R$ surface at 320 K results in the adsorption of a racemic mixture. Heating to 360 K raises the temperature to the point that desorption becomes rapid. The left panel of Figure 4 shows the results of experiments in which the Cu(643)$^{R\&S}$ surfaces at 360 K have been exposed to 0.03 L of either R-3-MCHO or racemic 3-MCHO using the doser and were then annealed at 360 K for 300 s before cooling. The conditions of the exposure allow adsorption at the kinks only and then allow some fraction of the adsorbed molecules to desorb into the vacuum. The amount of material remaining on the surface is then determined by TPD measurements.

First, concentrate on the TPD curves in Figure 4 labeled R/R and R/S which were obtained by exposing the Cu(643)$^{R\&S}$ surfaces to R-3-MCHO at 360 K and then allowing some

fraction to desorb during annealing for 300 s at 360 K. As illustrated in the TPD spectra of Figure 1, R-3-MCHO has a higher adsorption energy on the Cu(643)$^S$ surface than on the Cu(643)$^R$ surface. Therefore, its rate of desorption at a given temperature is lower on the Cu(643)$^S$ surface than on the Cu(643)$^R$ surface. This is verified by the fact that after adsorption and then desorption at 360 K there is more R-3-MCHO remaining on the Cu(643)$^S$ surface than on the Cu(643)$^R$ surface. In fact, the amount of R-3-MCHO remaining on the Cu(643)$^S$ surface is almost 10 times that remaining on the Cu(643)$^R$ surface.

Next, concentrate on the curves labeled Rac/R and Rac/S in Figure 4. These were obtained by exposing the Cu(643)$^{R\&S}$ surfaces to racemic 3-MCHO at 360 K and then allowing some fraction to desorb during annealing for 300 s at 360 K. The racemic mixture has no net chirality, and so its properties should be independent of the chirality of the surface. This is verified by the fact that the TPD curves in Figure 4 labeled Rac/R and Rac/S are almost identical, indicating that the same amount of 3-MCHO has been left on both the Cu(643)$^R$ surface and the Cu(643)$^S$ surface.

Finally, it is important to note that exposure of racemic 3-MCHO to the Cu(643)$^R$ surface leaves almost 4 times as much adsorbed 3-MCHO as does exposure of R-3-MCHO to the Cu(643)$^R$ surface. Under the conditions of the experiment, however, the Cu(643)$^R$ surface exposed to the racemic 3-MCHO at 360 K begins with only half as much adsorbed R-3-MCHO as the Cu(643)$^R$ surface exposed to pure R-3-MCHO. Therefore, the amount of R-3-MCHO left on the Cu(643)$^R$ surface after exposure to racemic 3-MCHO and annealing at 360 K for 300 s must be less than or equal to the amount left after adsorption and annealing of pure R-3-MCHO. In other words, of the

3-MCHO left on the Cu(643)$^R$ surface after exposure to racemic 3-MCHO (Figure 4, Rac/R), the fraction attributable to R-3-MCHO must be less than that indicated by the TPD curve labeled R/R. The logical conclusion is that the remainder, which would be measured by the difference between the Rac/R and R/R TPD curves, must be due to S-3-MCHO on the surface. The mixture left on the surface must be composed of at least 75% S-3-MCHO and less than 25% R-3-MCHO. In reality, the Cu(643)$^R$ exposed to the racemic mixture at 360 K began with only half the R-3-MCHO adsorbed by exposure to the pure R-3-MCHO. Thus, the amount of R-3-MCHO remaining on the surface after adsorption and annealing of the racemic 3-MCHO on the Cu(643)$^R$ surface might be as little as 12.5% of the 3-MCHO in the Rac/R TPD curve. This then is the first evidence of an enantioselective kinetic separation of a racemic compound on a naturally chiral metal surface! In a single adsorption/desorption step, the Cu(643)$^S$ surface has purified the racemic 3-MCHO such that the remainder adsorbed on the surface has an enantiomeric excess of at least ee = 50%.

There is one caveat to the above experiment that must be examined before settling on the conclusion that these experiments have demonstrated a true enantioselective separation. It is possible there are specific interactions between adsorbed R- and S-enantiomers of 3-MCHO that stabilize R−S complexes on the surface. If these interactions were not present when R-3-MCHO is adsorbed alone, they could give rise to the excess 3-MCHO on the surface following adsorption of the racemic 3-MCHO and annealing at 360 K. Several experiments suggest that there are no such R−S interactions when the racemic mixture is adsorbed. First, the TPD spectra of the racemic 3-MCHO adsorbed on the Cu(643)$^{R\&S}$ surfaces at low temperatures are almost identical to those of the pure R-3-MCHO on the Cu(643)$^{R\&S}$ surfaces. The peak desorption temperature of racemic 3-MCHO from the kinks lies roughly midway between the desorption temperatures of R-3-MCHO from the R- and S-kinks.[12] Second, the average of the FT-IRAS spectra of the R-3-MCHO adsorbed at the kinks on the Cu(643)$^{R\&S}$ surfaces is identical to the spectrum of the racemic mixture on either the Cu(643)$^R$ or the Cu(643)$^S$ surface. This again suggests that there are no specific interactions between the two enantiomers when coadsorbed.

Finally, we have performed a control experiment to detect the possible presence of specific R−S interactions under conditions analogous to those used to demonstrate an enantioselective kinetic separation on the Cu(643)$^{R\&S}$ surfaces. These measurements were done using the achiral Cu(533) surface which exposes straight (100) step edges. Because its structure is achiral, adsorption and desorption of R-3-MCHO or racemic 3-MCHO cannot be influenced by enantiospecificity. Differences in the adsorption of R-3-MCHO and racemic 3-MCHO could then be attributed to R−S interactions in the racemic mixture which are absent in the pure R-3-MCHO. Racemic 3-MCHO and R-3-MCHO were exposed to the Cu(533) surfaces at 330 K and then annealed in a vacuum at 330 K for 300 s. As indicated in Figure 1, the 3-MCHO will adsorb at the straight step edges, but at 330 K desorption is still quite rapid. Following these treatments, the 3-MCHO remaining on the surface was
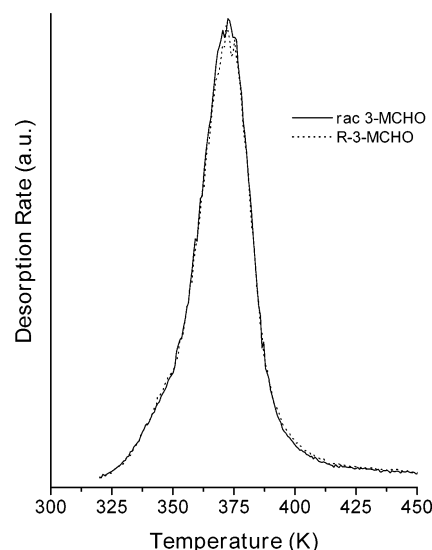


**Figure 5.** TPD of 3-MCHO from achiral Cu(533) following exposure to racemic 3-MCHO and R-3-MCHO at 330 K and annealing at 330 K for 300 s. The two TPD traces reveal identical, submonolayer coverages of 3-MCHO remaining adsorbed on the surface. Because the surface is achiral, there are no enantiospecific interactions between the adsorbate and the surface. The only enantiospecific interactions possible are those between adsorbed enantiomers of 3-MCHO. The fact that the coverages left adsorbed on the Cu(533) surface are identical indicates that there are no detectable differences between the R−S interactions of the racemic mixture and the R−R interactions of the pure R-3-MCHO.

detected by TPD. Figure 5 shows the resulting TPD spectra of 3-MCHO from the Cu(533) surface and demonstrates that the amounts remaining on the surface are identical. The implication of these experiments is that there are no R−S interactions present in adsorbed racemic 3-MCHO and thus that its adsorption and desorption behavior on the Cu(643)$^{R\&S}$ surfaces can be considered to be that of an "ideal" mixture of R- and S-3-MCHO. In summary, the data presented in Figure 4 provide the first experimental evidence for a kinetic separation of racemic 3-MCHO on the Cu(643)$^{R\&S}$ surfaces.

## 5. Conclusions

Stepped-kinked surfaces such as Cu(643)$^{R\&S}$ are known to be chiral and have been shown to exhibit enantiospecific properties when interacting with enantiomerically pure chiral compounds such as R-3-MCHO. The TPD spectra of 3-MCHO from the Cu(643)$^{R\&S}$ surfaces resolve three distinct desorption features which are attributable to desorption from terraces (230 K), straight steps edges (345 K), and chiral kinks (385 K). The desorption feature at 385 K which exhibits enantiospecificity has been shown to be that attributable to desorption from the kinks. Finally, we have reported the first evidence for the enantioselective separation of a racemic mixture (3-MCHO) into enantiomerically purified components on a naturally chiral metal surface.